Characterization of the impact of oxygen concentration on the alumina cloud surrounding a burning aluminum droplet

Hugo Keck[a], Christian Chauveau[a], Guillaume Legros[b], Stany Gallier[c],
Fabien Halter[a] and Guillaume Dayma[a]
[a]ICARE-CNRS, [b]Institut d'Alembert, [c] ArianeGroup
[a]Orléans, 45100, France, [b]Paris, 75005, France, [c]Vert-le-Petit, 91710, France

1 Introduction

The high energetic density of aluminum makes it a relevant choice as an energetic additive in the propulsion field. Mainly added to solid fuels, its use improves the global performance of the rocket due to its high combustion temperature. Moreover, aluminum is gaining consideration as a potential clean energy carrier. Indeed, its availability, ease of transportation or capacity to recycle are characteristics that are sought after [1]. During the combustion of an aluminum particle in the gas phase regime, aluminum reacts with the available oxygen in a region separate from the particle, resulting in the formation of alumina through a highly exothermic reaction. Upon formation, alumina instantly condenses into nanodroplets. These droplets can then coagulate or aggregate upon cooling, forming the primary condensed combustion products (CCPs). In the military or space explorations fields, characterizing these CCPs is essential, as it directly affects rocket efficiency through thermoacoustic oscillations or two-phase ejection losses. This characterization is also vital for aluminum recycling, as alumina must be recovered and reduced to form aluminum again. Therefore, assessing the characteristics of alumina around a burning aluminum droplet is of utmost importance. While numerical studies remain scarce and present discrepancies in the results, the methods developed in [2] and [3] allow for the non-intrusive determination of in situ alumina size, concentration, temperature and gaseous emission profiles during the combustion of a levitating aluminum droplet in a chosen environment. While results in the case of air have already been published [2, 3], the impact of oxygen concentration of the combustion parameters needs to be understood. In this work, a light extinction method (LEM) combined with a modulated absorption emission (MAE) method as developed in [2,3] is applied to the case of an aluminum droplet burning in an O_2/Ar mixture at 1 bar. To grasp the impact of oxygen concentration, the results for a $21\%O_2/79\%Ar$(vol.) are compared to those for a $30\%O2/70\%Ar$(vol.) mixture. The size, concentration and temperature profiles of alumina nanoparticles are obtained for a 70 micron diameter aluminum particle. Section 2 and 3 respectively briefly introduce the experimental setup and the associated method, section 4 discusses the results and section 5 brings a conclusion to this work.

2 Experimental setup

The combustion of a levitating aluminum particle is made possible through the use of an electrodynamic levitator, placed in a combustion chamber. In the chamber previously filled with a selected mixture at 1

Correspondence to: hugo.keck@cnrs-orleans.fr

bar, charged aluminum particles are introduced into the levitator with a syringe, and a chosen particle is isolated by adequately tuning the tensions of the electrodes of the levitator as well as the frequency of the alternating current. The particle is then impacted from both sides by a 50W CO_2 laser until ignition of the particle. Combustion emissions are recorded by photomultipliers that allow shutting the laser off upon ignition based on an arbitrary threshold. Self-sustained combustion of an isolated levitating particle is thus achieved. A high-speed color camera PHANTOM T-2410 is coupled to a teleobjective QUESTAR QM100 and a triple band filter (450 nm, 530 nm, 630 nm) to record the particle during combustion with a frequency of 15 kHz and a resolution of about 1.3 microns per pixel. To implement the LEM, a LED SOLIS-3C is utilized as a backlight, pulsed at half the camera's frequency. This allows for the difference of two consecutive images during processes, to suppress flame emission in order to correctly assess absorption of the LED emission by the alumina nanoparticles. The use of a triple band filter makes it possible to retrieve the combustion emissions, at the wavelengths of the filter, on the RGB matrices of the camera. With the use of a black body calibration, these three matrices allow for the determination of temperature profiles. The complete experimental setup is represented in Fig. 1. Note that the combustion chamber is not represented for clarity.

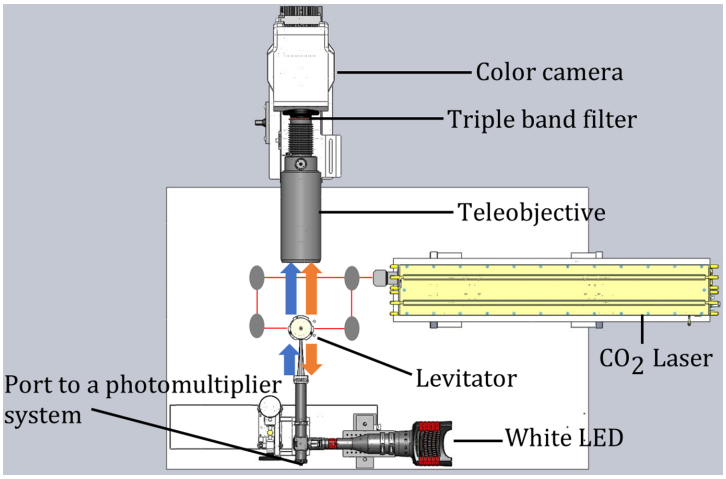

Figure 1: Top view of the experimental apparatus allowing for a LEM combined with a MAE method. A single aluminum droplet (not depicted) is located inside the levitator. Blue arrows represent LED emissions. Orange arrows represent combustion emissions. Red lines represent the laser path.

3 Method

The experimental apparatus introduced in the previous section allows for the observation of the aluminum particle during the combustion process and an image captured by the camera is displayed in Fig. 2. In this section, the method that allows the assessment of the alumina size, concentration and temperature profiles will only be briefly described, as it is available in the literature [2, 3].

The first part of the global method consists in the application of a LEM. A hypothesis is made that the only attenuating species in the cloud is the condensed alumina and the gaseous phases are considered to be transparent. Under this assumption, the Beer-Lambert's law relates the optical depth τ of a medium for a wavelength λ to the volume fraction f_v of the attenuating species through the following equation:

$$\tau(\lambda) = \int_0^l \sigma(r(z), \lambda) \frac{f_v(z)}{4/3 \cdot \pi \cdot r(z)^3} dz$$

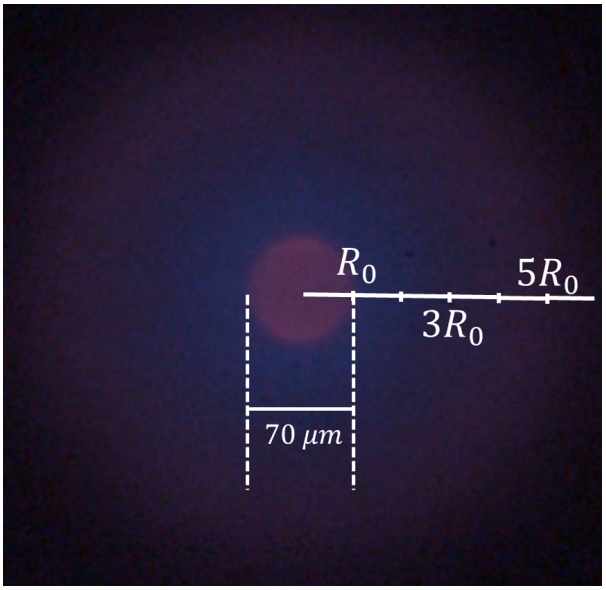

Figure 2: Image of a 70-micron aluminum particle burning in $30\%O_2/70\%Ar$ (vol.) mixture at 1 bar.

The length of the optical path is denoted as l and the alumina is considered as spheres of radius r. At a given wavelength and for a sphere of a given size, the Mie theory introduces the extinction cross section of this sphere $\sigma\,(r, \lambda)$, which can be computed with the knowledge of the optical properties of the material of the sphere. The optical depth is assessed using the LEM fully introduced in previous work [2] using the absorption of the LED through the oxide cloud. With the use of a deconvolution procedure, local optical depth is assessed (in opposition to optical depth integrated along the optical path) corresponding to local values of the right-hand side of the equation. Note that the radius of the alumina particles is not known and is required to assess the concentration profile of alumina. An optimization procedure has been developed in previous work to assess the size profile of alumina using the information of optical depth at the three wavelengths available. Upon application of this optimization procedure, the alumina size and concentration profiles are assessed. Note that optical depth is simply related to emissivity and thus, local emissivity of the cloud is also assessed and allows for the use of the MAE method. Indeed, in images recorded, such as the one presented in Fig 2, emission profiles within the cloud can easily be assessed and a deconvolution procedure can be applied to retrieve local emission profiles of the cloud at given wavelengths using the RGB matrices of the camera. As emissivity profiles are known, local emission profiles are divided by local emissivity profiles to evaluate local black body emission profiles. Profiles of R/G, R/B and G/B emissions can be obtained. A black body calibration of the camera has been performed to allow the association of emission ratios to the corresponding black body temperature. Note however that upon directly using calibration data to assess the temperature profile, unexpected results (T>8000K) are observed. Indeed, gaseous suboxides emit light in the blueish region of the visible spectrum [4] and thus alter the black body character of the emission ratios. An optimization procedure has been developed to split black body emissions from gaseous emissions based on a self-consistency procedure constrained by physical laws [3]. Through the application of this procedure, the temperature profile of alumina is assessed as well as the gaseous emission profiles for the three wavelengths of interest.

4 Results and discussion

Using the LEM, alumina size and concentration profiles are assessed and presented in Fig. 3 for both cases of interest. The temperature profiles, evaluated using the MAE method are shown with their respective 95% confidence interval in Fig 4. In the less oxygenated case, the alumina particle radius ranges from 140 nm to 100 nm, reaching this size at about 6 droplet radii. In conjunction, a maximum volume fraction of $1.5 \cdot 10^{-4}$ is observed at the droplet's surface. A second local maximum of $0.5 \cdot 10^{-5}$ is found near 5 droplet radii, closely matching the region of minimum size. In comparison, the most oxygenated case presents an alumina particle size ranging from 100 nm to 70 nm in radius, with a maximum volume fraction of about $1.2 \cdot 10^{-4}$ at the droplet's surface and a local maximum of $1.4 \cdot 10^{-5}$ at approximately 5.3 droplet radii. In both cases, alumina size increases near the droplet's surface due to the significant temperature gradient between the droplet and the flame region coupled to an increasing alumina concentration that favors alumina condensation and coalescence. On the other side of the size profile, the alumina growth is only observed in the less oxygenated case. As shown in Figs. 3, 4, alumina in the most oxygenated case remains denser and hotter at a greater distance from the droplet's surface compared to the less oxygenated case. It is assumed that if oxide particles growth, it settles too far from the droplet to be observed. In both cases, a significant alumina concentration is measured close to the droplet's surface. Although the gas phase regime is observed, with a flame clearly detached from the droplet's surface (see Fig. 2), heterogeneous surface reactions and reactions close to the surface can occur [8] due to the expected presence of oxygen or oxygen carriers [5] at this location of the cloud, leading to possible alumina production. Alumina particle back diffusion towards the aluminum droplet is also possible through phoretic motions [6]. The maximum simulated speed for the phoretic flow is of about 18 m/s versus 16 m/s for the Stefan flow [6], giving a ratio of the drag force induced by the phoretic motions to that of the Stefan flow on alumina droplets of about 1.27. The current method cannot determine the origin of the alumina near the droplet's surface. Alumina concentration in the $30\%O_2/70\%Ar$ (vol.) mixture is evaluated to be higher than in the $21\%O_2/79\%Ar$ (vol.) mixture at nearly all points in the cloud. The lower combustion time [7] and higher temperature from Fig. 4 in the most oxygenated case lead to a greater evaporation rate than in the less oxygenated case. The greater production of gaseous aluminum results in increased alumina production as observed in the experiments.

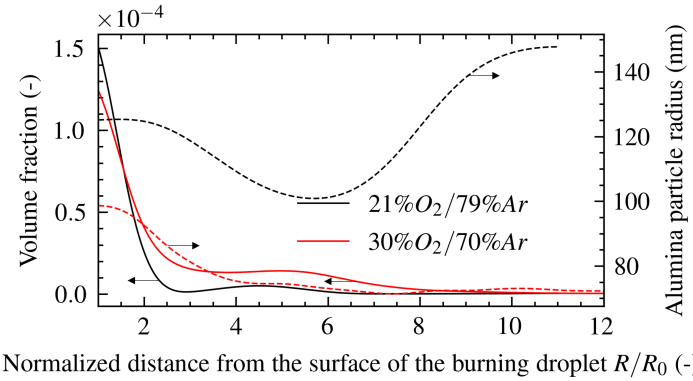

Figure 3: Alumina concentration (continuous) and size (dashed) profiles in the case of an aluminum particle of radius $R_0 = 35\mu m$ burning in $30\%O_2/70\%Ar$ (vol.) (red) and $21\%O_2/79\%Ar$ (vol.) (black) mixtures at 1 bar.

From Fig. 4, the surface temperatures of the aluminum droplet for the $30\%O_2$ case and the $21\%O_2$ are assessed at 2700 K (approaching the boiling temperature of aluminum) and 2300 K respectively. Close to the droplet's surface, both temperature profiles show a minimum temperature. As introduced by Bucher [9] with the reaction of aluminum with nitrogen, endothermic reactions can occur within the oxide cloud.

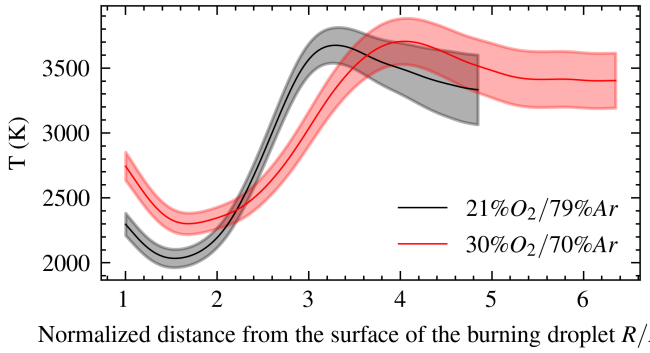

Figure 4: Alumina temperature profile in the case of an aluminum particle of radius $R_0 = 35\mu m$ burning in $30\%O_2/70\%Ar$ (vol.) (red) and $21\%O_2/79\%Ar$ (vol.) (black) mixtures at 1 bar.

The presented methodology allows for the assessment of a normalized gaseous emission profile shown in Fig. 5. The gaseous emissions being mostly attributed to the presence of AlO [3], the minimum temperature is located slightly closer to the droplet than the apparent AlO maximum concentration. Saba et. al. [10] identified the main reaction path for aluminum oxidation and found that AlO mainly reacts with itself to form Al_2O releasing an oxygen atom O. Once Al_2O is formed, its main oxydation reaction is identified to be $Al_2O + O_2$ forming Al_2O_2 and an oxygen atom O through an endothermic reaction. Non-prevailing reactions with dioxygen to form $Al + AlO_3$, $Al_2O_2 + O$ or $AlO + AlO_2$ are also endothermic. Other reactions of Al_2O with monoatomic oxygen O to form $2AlO$ or $Al + AlO_2$ are also identified as endothermic. Therefore, it is assumed that this location in the cloud is the main reaction zone of Al_2O with O_2 and O. Note that gaseous emissions at greater droplet radii might be electronic emissions detected as a gaseous phase [3]. For locations further from the droplet's surface, oxide temperature increases to reach a maximum at what is arbitrarily determined as the standoff ratio of the flame. In the most oxygenated environment, the maximum temperature of 3705 K is evaluated at 4 droplet radii, compared to a maximum temperature of 3675 K at 3.3 droplet radii for the less oxygenated case. Although the maximum temperatures for both cases are not significantly different, the maximum temperature is established at the location of alumina production (and condensation) due to the high exothermicity of this reaction. The location of this reaction is influenced by a complex interplay between species diffusion (and thus mixture composition) and the rate of gaseous aluminum production. Assuming both mixtures have relatively similar diffusion properties, given the close flame temperatures, the increase in standoff ratio for the most oxygenated mixture can be explained by the greater amount of oxygen diffusing to the droplet's surface, thereby increasing the share of surface reactions. With more in exothermic surface reactions, the evaporation rate of aluminum rises, which in turn increases the Stefan flow from the droplet, leading to a higher standoff ratio. This consideration supports the observed increase in the droplet temperature with higher oxygen concentration.

5 Conclusion

The in situ study of the CCPs produced by a single burning aluminum droplet is facilitated by using an electrodynamic levitator. To understand the impact of oxygen on the combustion process, recently developed methods are applied to aluminum burning in two mixtures with different oxygen concentrations: $30\%O_2/70\%Ar$ (vol.) and $21\%O_2/79\%Ar$ (vol.). In the less oxygenated mixture, alumina size ranges between 100 nm and 140 nm in radius, with a local maximum volume fraction of $0.5 \cdot 10^{-5}$. In comparison, the most oxygenated mixture shows a smaller alumina size ranging from 70 nm to 100 nm in radius and a higher concentration with a local maximum of $1.4 \cdot 10^{-5}$. Additionally, temperature

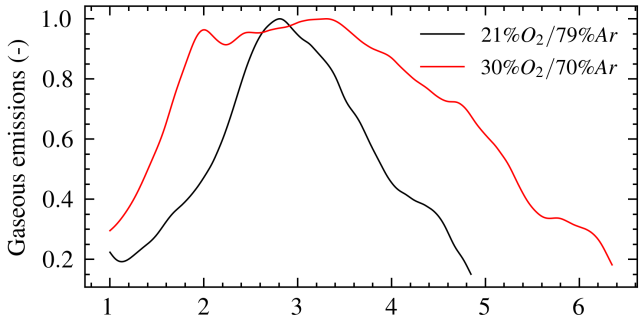

Figure 5: Normalized gaseous emission profile in the case of an aluminum particle of radius $R_0 = 35\mu m$ burning in $30\%O_2/70\%Ar$ (vol.) (red) and $21\%O_2/79\%Ar$ (vol.) (black) mixtures at 1 bar.

profiles are assessed, revealing a slightly higher maximum temperature for the most oxygenated mixture at 3705 K, compared to 3675 K for the less oxygenated mixture. These temperatures located at different standoff ratios, are explained by the consideration of surface reactions and the influence of the Stefan flow.

References

[1] Bergthorson JM, Goroshin S, Soo MJ, Julien P, Palecka J, Frost DL, Jarvis DJ. (2015). Direct combustion of recyclable metal fuels for zero-carbon heat and power. Appl. Energy. 160: 368.

[2] Keck H, Chauveau C, Legros G, Gallier S, Halter F. (2024). New experimental method for the simultaneous determination of concentration and size profiles of condensed combustion products around a burning aluminum droplet. Combust. Flame. 268: 113616.

[3] Keck H, Chauveau C, Legros G, Gallier S, Halter F. (To be published). Temperature field measurement of a burning aluminum droplet. Combust. Flame.

[4] Dabos M, Tran K, Lecysyn N, Baudin G, Genetier M, Ranc I, Serio B. (2019). Investigation of alumina's emission in the deflagration of gas-aluminum particles mixtures. Europyro, Tours, France.

[5] Beckstead M. (2003). A summary of aluminum combustion. NATO RTO-EN-023.

[6] Gallier S, Braconnier A, Godfroy F, Halter F, Chauveau C. (2021). The role of thermophoresis on aluminum oxide lobe formation. Combust. Flame. 228: 142

[7] Gill RJ, Badiola C, Dreizin EL. (2010). Combustion times and emission profiles of micron-sized aluminum particles burning in different environments. Combust. Flame. 157: 2015

[8] Villard J. (2024). Numerical simulation of aluminum particle combustion. PhD Thesis, Université de Toulouse.

[9] Bucher P, Yetter RA, Dryer FL, Parr TP, Hanson-Parr DM. (1998). PLIF species and ratiometric temperature measurements of aluminum particle combustion in O2, CO2 and N2O oxidizers, and comparison with model calculations. Symp. (Int.) Combust. 27: 2421

[10] Saba M, Kato T, Oguchi T. (2021). Reaction modeling study on the combustion of aluminum in gas phase: The Al + O2 and related reactions. Combust. Flame. 225: 535